Ru(II) Water Oxidation Catalysts with 2,3-bis(2-Pyridyl)Pyrazine and tris(Pyrazolyl)Methane Ligands: Assembly of Photo- and Catalytic-Active Subunits in a Dinuclear Structure

Alice de Palo, Giuseppina La Ganga, Francesco Nastasi, Massimo Guelfi, Marco Bortoluzzi, Guido Pampaloni, Fausto Puntoriero, Sebastiano Campagna and Fabio Marchetti

Supporting Information

Table of contents *Page*

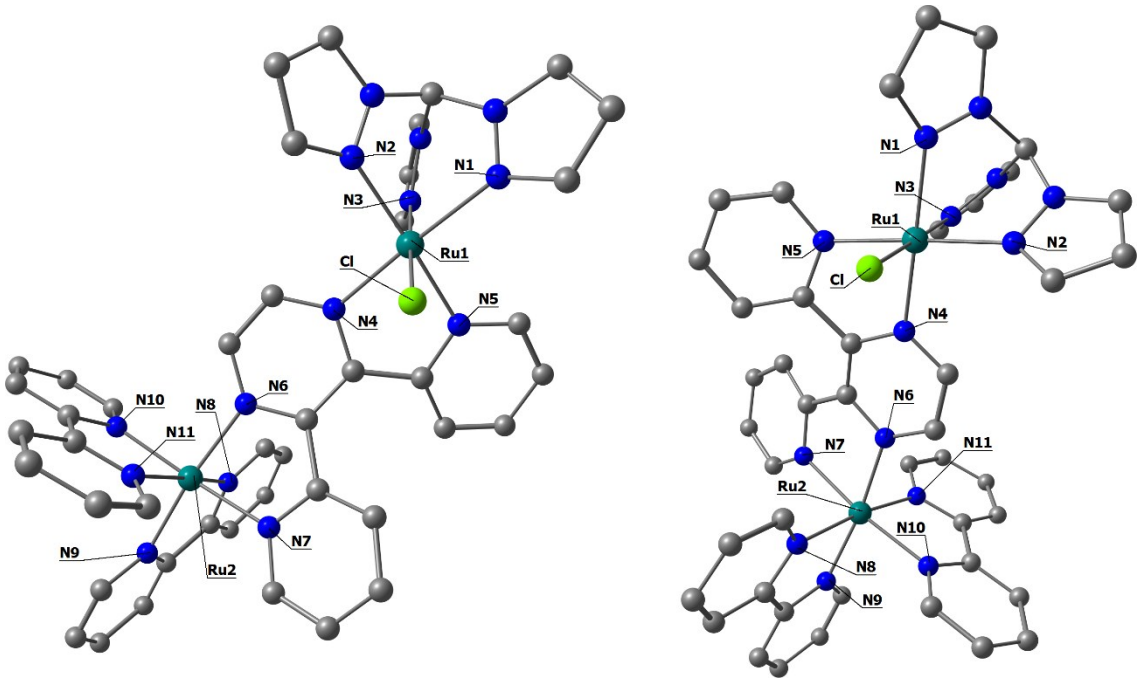

[3A]$^+$ **[3B]$^+$**

Figure S1. DFT-optimized geometries of the diastereoisomers [**3A**]$^{3+}$ and [**3B**]$^{3+}$ (C-PCM/ωB97X calculations, dichloromethane as continuous medium). Colour map: Ru, dark green; Cl, light green; N, blue; C, grey. Hydrogen atoms are omitted for clarity.

Selected computed lengths (Å) for [**3B**]$^{3+}$: Ru1-Cl 2.414; Ru1-N1 2.111; Ru1-N2 2.110; Ru1-N3 2.093; Ru1-N4 2.061; Ru1-N5 2.090; Ru2-N6 2.089; Ru2-N7 2.096; Ru2-N8 2.106; Ru2-N9 2.096; Ru2-N10 2.098; Ru2-N11 2.104. Selected computed angles (°) for [**3B**]$^{3+}$: Cl-Ru1-N1 91.6; Cl-Ru1-N2 90.9; Cl-Ru1-N3 176.4; Cl-Ru1-N4 89.8; Cl-Ru1-N5 87.4; N6-Ru2-N7 77.9; N6-Ru2-N8 96.0; N6-Ru2-N9 172.5; N6-Ru2-N10 97.4; N6-Ru2-N11 89.7.

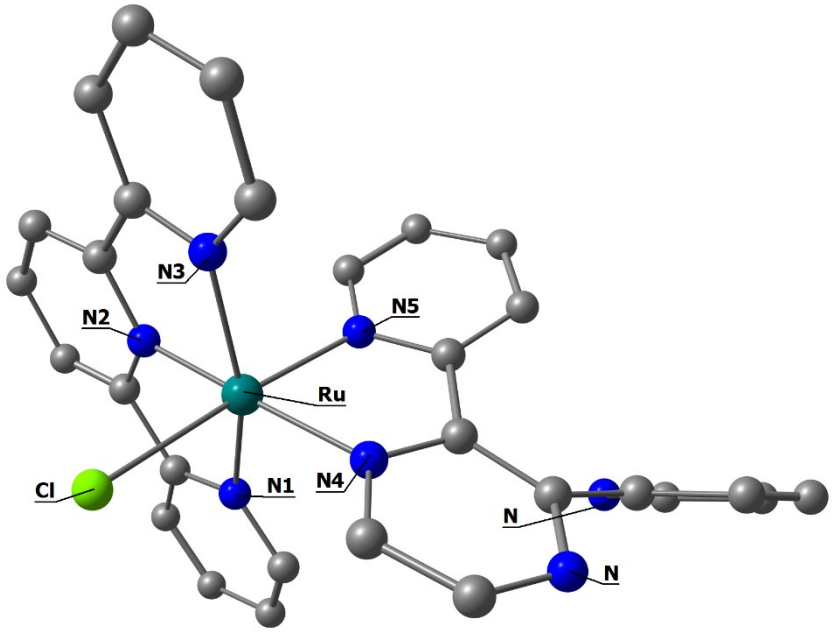

Figure S2. DFT-optimized geometry of [**1**]$^{+}$ (C-PCM/ωB97X calculations, water as continuous medium). Colour map: Ru, dark green; Cl, light green; N, blue; C, grey. Hydrogen atoms are omitted for clarity.

Selected computed lengths (Å) for [**1**]$^{+}$: Ru-Cl 2.414; Ru-N1 2.108; Ru-N2 1.984; Ru-N3 2.103; Ru-N4 2.100; Ru-N5 2.076. Selected computed angles (°) for [**1**]$^{+}$: Cl-Ru-N1 90.0; Cl-Ru-N2 87.9; Cl-Ru-N3 89.8; Cl-Ru-N4 95.2; Cl-Ru-N5 172.7.

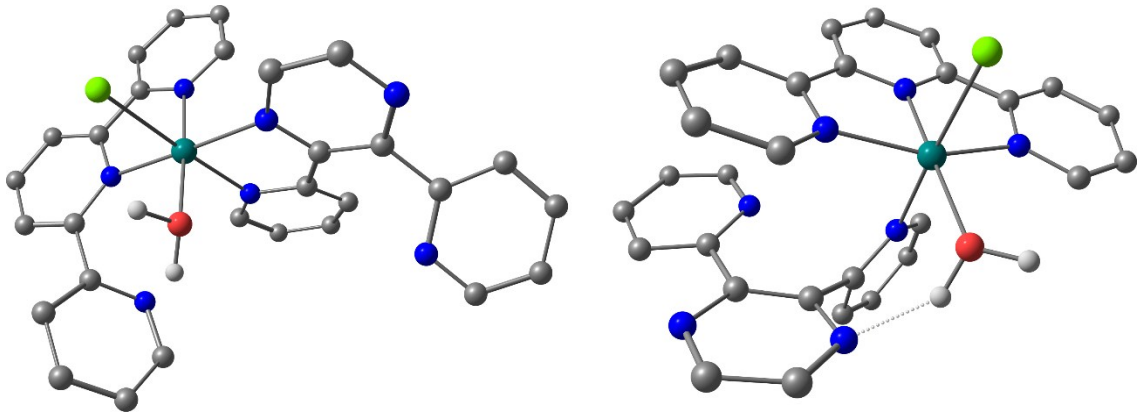

$[\mathbf{1}^{\mathbf{W}}\mathbf{A}]^+$ $[\mathbf{1}^{\mathbf{W}}\mathbf{B}]^+$

Figure S3. DFT-optimized geometry of $[\mathbf{1}^{\mathbf{W}}\mathbf{A}]^+$ and $[\mathbf{1}^{\mathbf{W}}\mathbf{B}]^+$ (C-PCM/ωB97X calculations, water as continuous medium). Colour map: Ru, dark green; Cl, light green; N, blue; C, grey. Hydrogen atoms. except for those of coordinated water, are omitted for clarity.

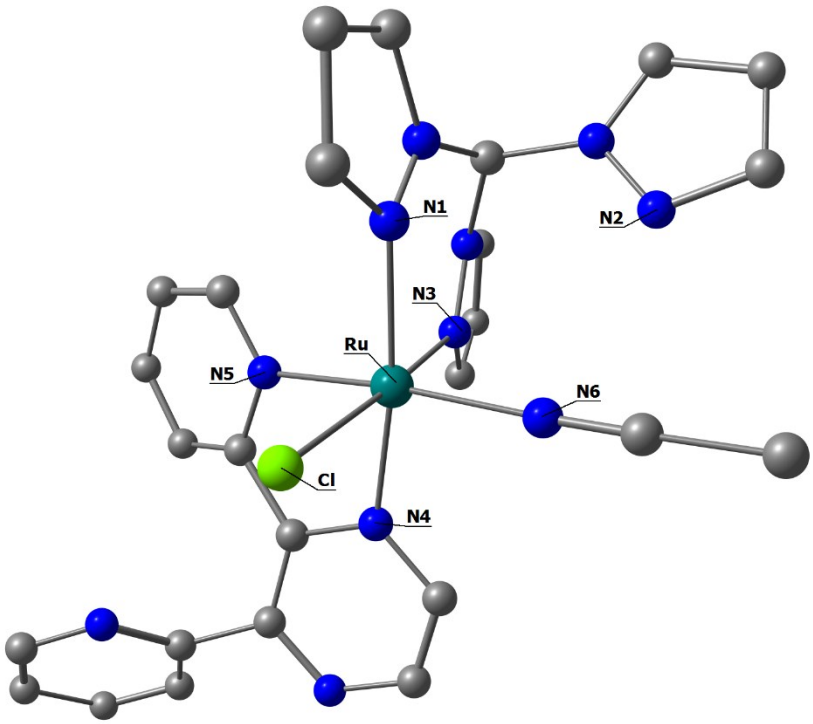

Figure S4. DFT-optimized geometry of $[\mathbf{2}^{\mathbf{AN}}]^{+}$ (C-PCM/ωB97X calculations, acetonitrile as continuous medium). Colour map: Ru, dark green; Cl, light green; N, blue; C, grey. Hydrogen atoms are omitted for clarity.

Selected computed lengths (Å) for $[\mathbf{2}^{\mathbf{AN}}]^{+}$: Ru-Cl 2.444; Ru-N1 2.116; Ru-N3 2.103; Ru-N4 2.070; Ru-N5 2.081; Ru-N6 2.042. Selected computed angles (°) for $[\mathbf{2}^{\mathbf{AN}}]^{+}$: Cl-Ru-N1 91.7; Cl-Ru-N3 176.5; Cl-Ru-N4 85.4; Cl-Ru-N5 90.5; Cl-Ru-N6 89.3.

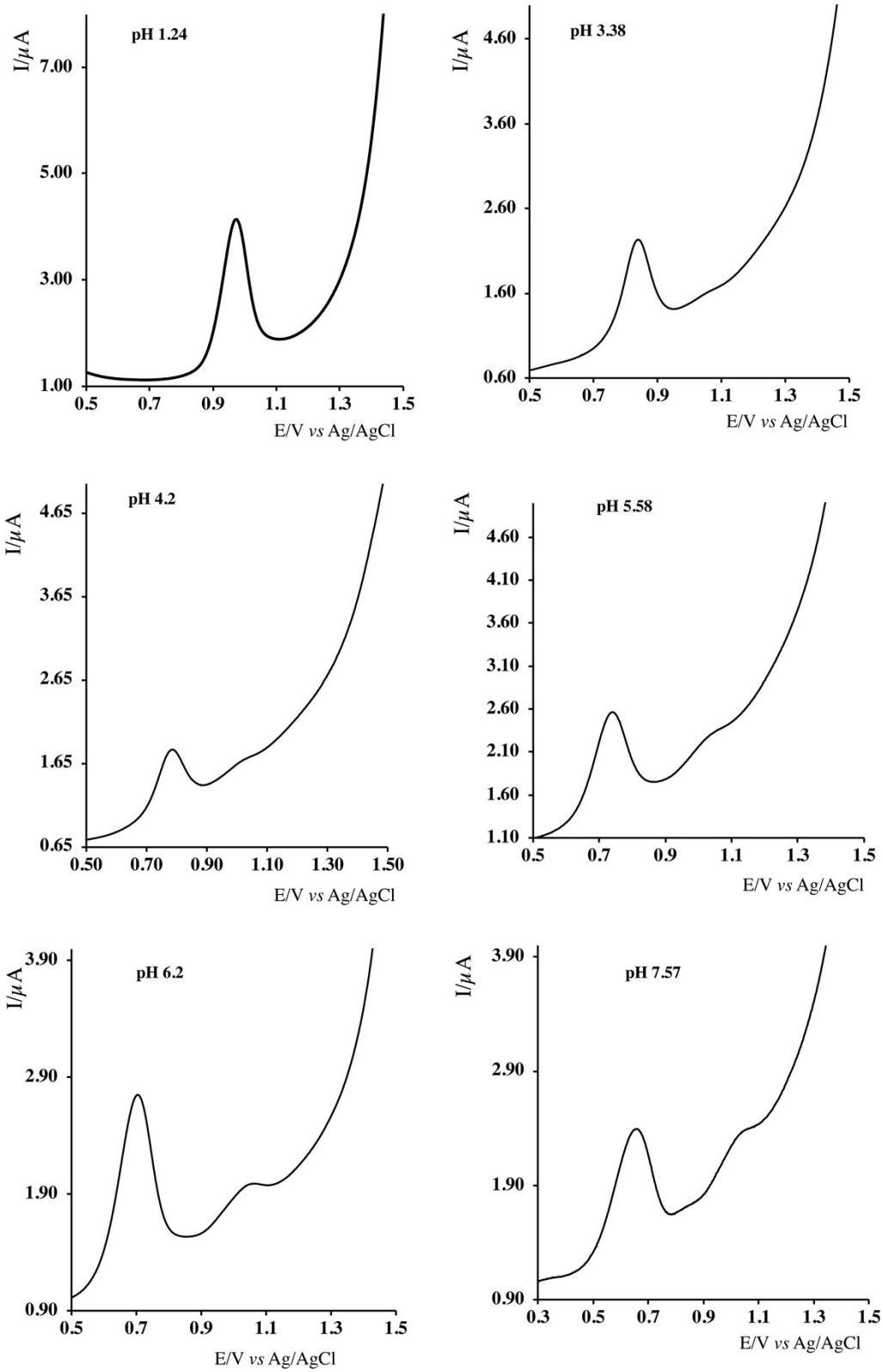

Figure S5. DPV of [**1**]PF_6 (1.2 x 10^{-4} M) at different pH that were adjusted by adding small amounts of NaOH(sol) to a 0.1 M $HClO_4$ solution and determined by a pH-meter. Glassy carbon was used as working electrode, platinum as counter and Ag/AgCl as reference. Scan rate 20 mV/s.

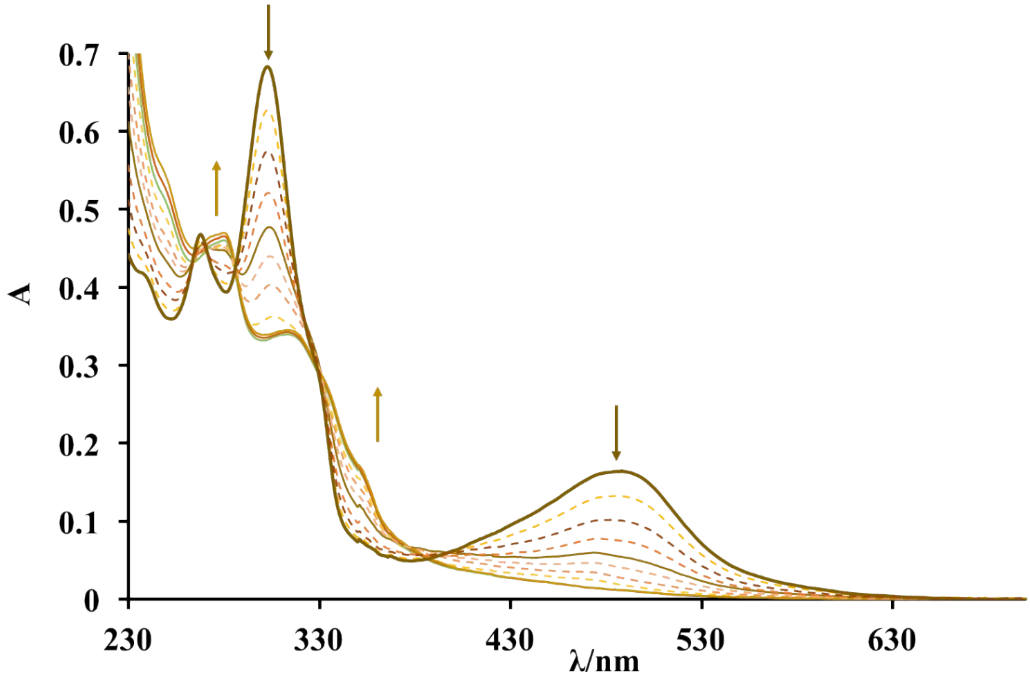

Figure S6. Spectral changes upon addition of CAN (5×10^{-3}M) to a solution of [**1**]PF_6 (2×10^{-5}M) in $HClO_4$ 0.1 M. Solid lines refer to [CAN]/[**1**] ratio 0, 1 and 2 respectively.

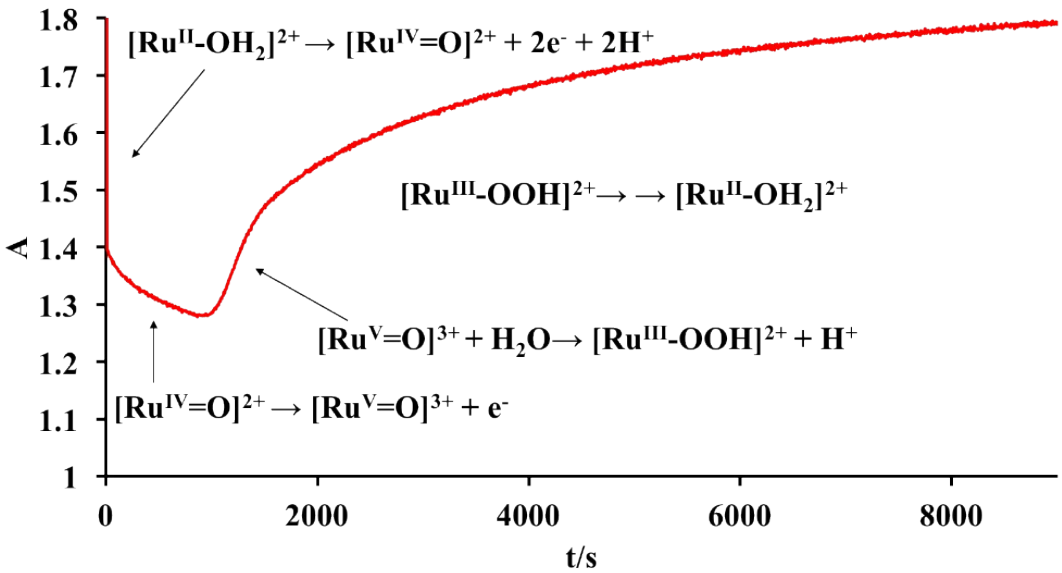

Figure S7. Absorbance changes at 305 nm upon addition of three equivalents of CAN to a solution of [**1**]PF_6 ($5x10^{-5}$M) in $HClO_4$ 0.1 M.

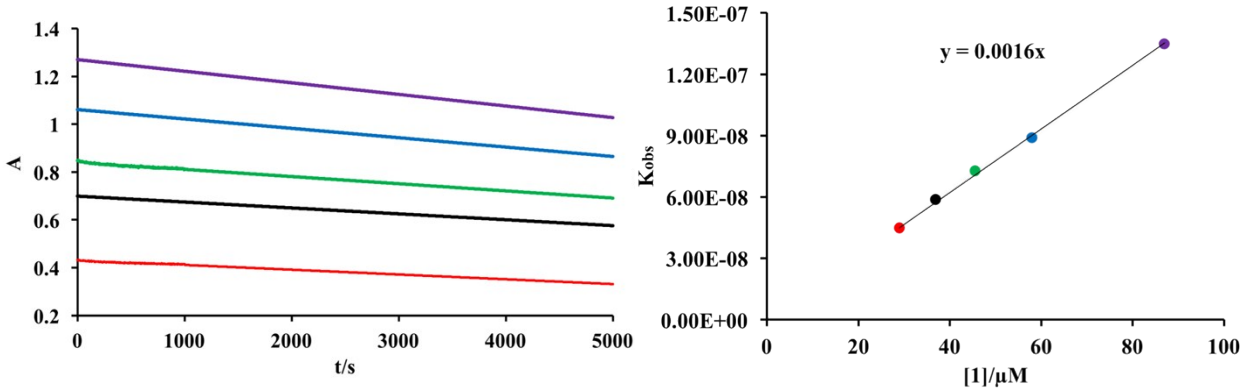

Figure S8. Left side: Absorbance changes at 360 nm upon addition of 30 equivalents of CAN to a solution of [**1**]PF_6 at different concentrations (29, 37, 46, 58 e 87 µM) in $HClO_4$ 0.1 M. Right side: k_{obs} *vs* catalyst concentration.

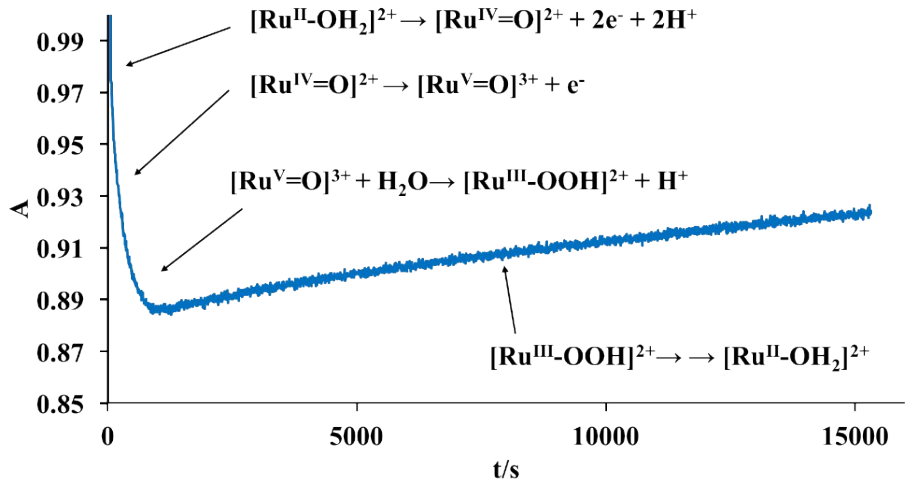

Figure S9. Absorbance changes at 305 nm upon addition of 3 equivalents of CAN to a solution of [**2**]Cl ($5x10^{-5}$M) in $HClO_4$ 0.1 M.

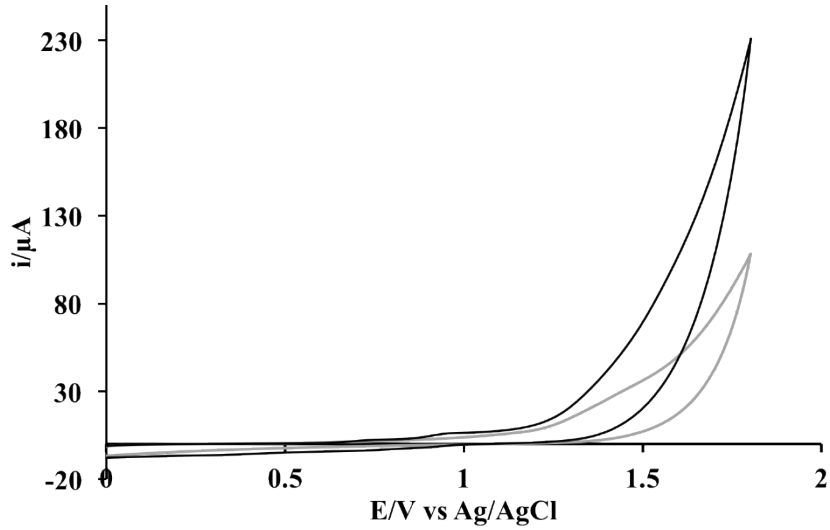

Figure S10. Cyclic voltammograms of [**3**][PF_6]$_3$ (black line) in the range 0.0-2.0 V *vs* Ag/AgCl in 1:1 (v/v) acetonitrile/phosphate buffer (pH 7) (glassy carbon working electrode, scan rate of 50 mV/s). In grey CV of solvent is reported.

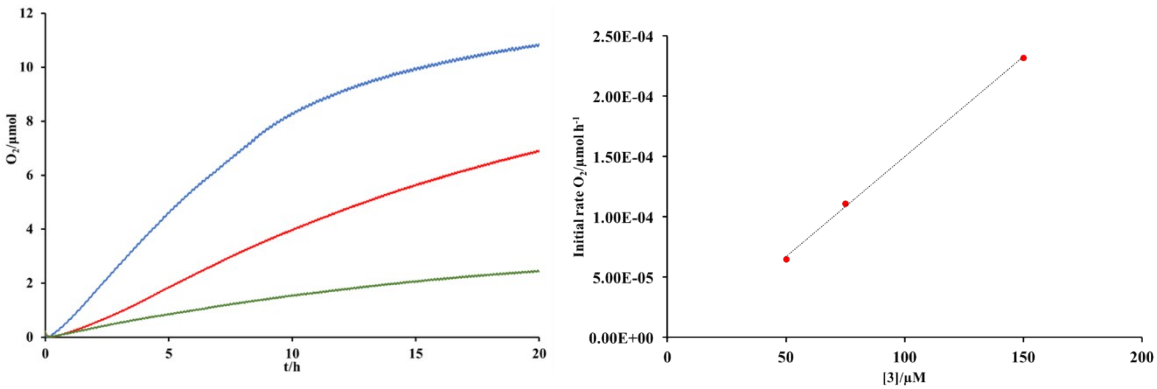

Figure S11. Left side: O_2 evolution *vs* time at different concentration of [**3**][PF_6]$_3$ in $HClO_4$ 0.1 M, in presence of CAN (200 mM); Right side: Initial rate of O_2 production as function of catalyst concentration ([**3**][PF_6]$_3$) (50, 75 and 150 µM).

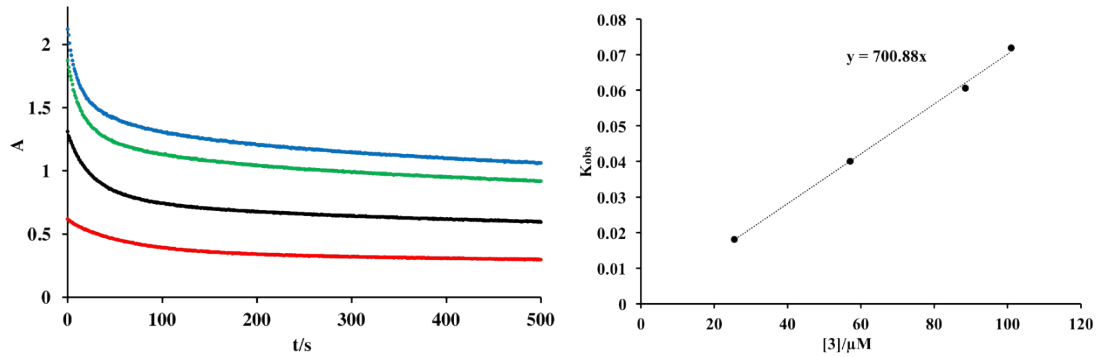

Figure S12. Left side: Absorbance changes at 360 nm upon addition of 30 equivalent of CAN to a solution of [**3**][PF_6]$_3$ at different concentrations (26, 58, 89 e 100 µM) in $HClO_4$ 0.1 M; right side: k_{obs} *vs* catalyst concentration (3).

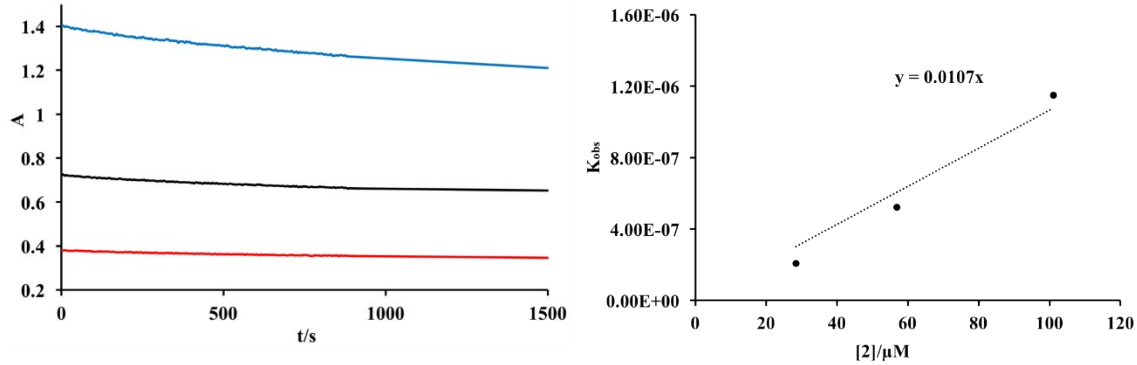

Figure S13. Left side: Absorbance changes at 360 nm upon addition of 30 equivalent of CAN to a solution of [**2**]Cl at different concentrations (28, 57,100 µM) in $HClO_4$ 0.1 M; right side: k_{obs} *vs* catalyst concentration (2).

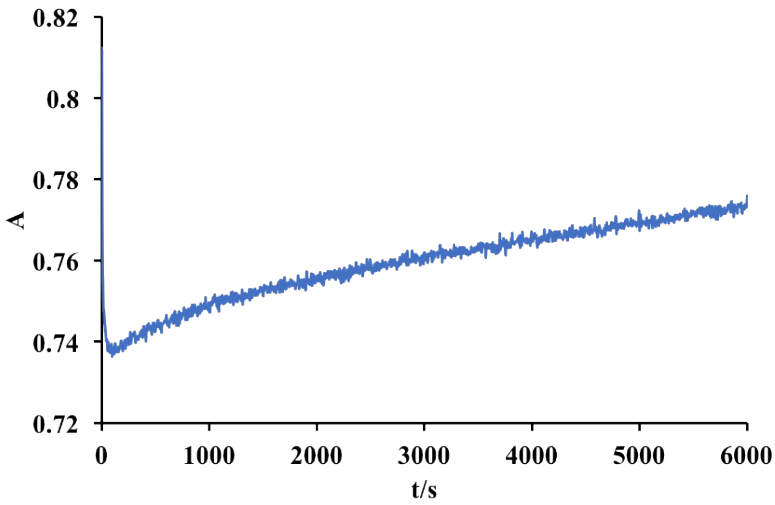

Figure S14. Absorbance changes at 305 nm upon addition of 3 equivalents of CAN to a solution of [**3**][PF_6]$_3$ (5x10^{-5}M) in $HClO_4$ 0.1 M.

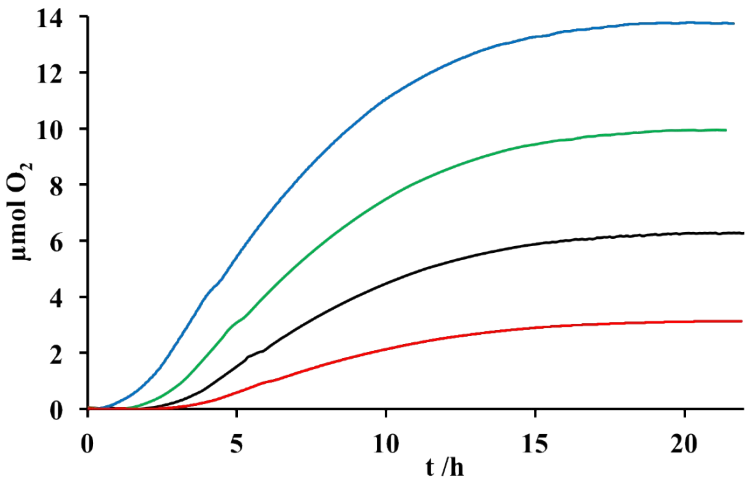

Figure S15. O_2 evolution *vs* time at different concentrations (47, 94, 145 e 190 µM) of [**1**]PF_6 in $HClO_4$ 0.1 M, in the presence of CAN (200 mM).

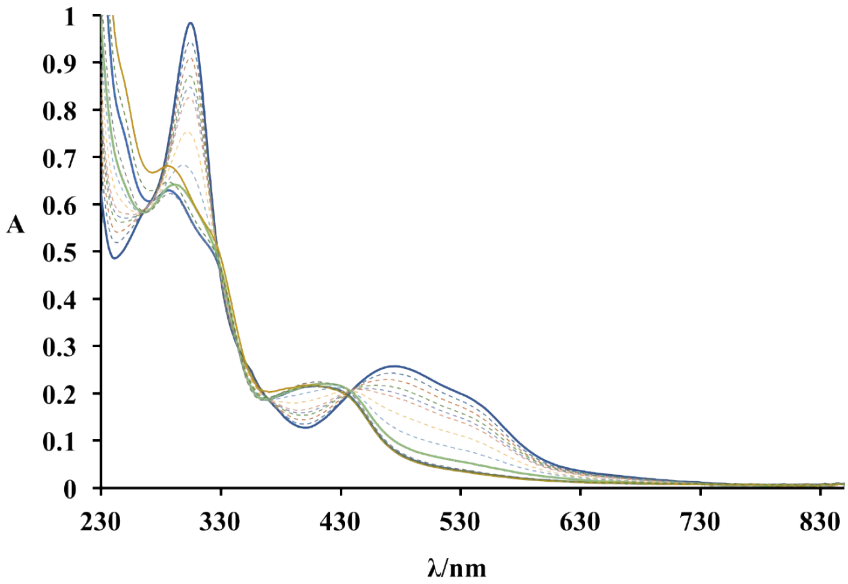

Figure S16. Spectral changes upon addition of CAN (5×10^{-3}M) to a solution of [**2**]Cl (2×10^{-5}M) in $HClO_4$ 0.1 M. Solid lines refer to [CAN]/[**1**] ratios 0, 1 and 2 respectively.

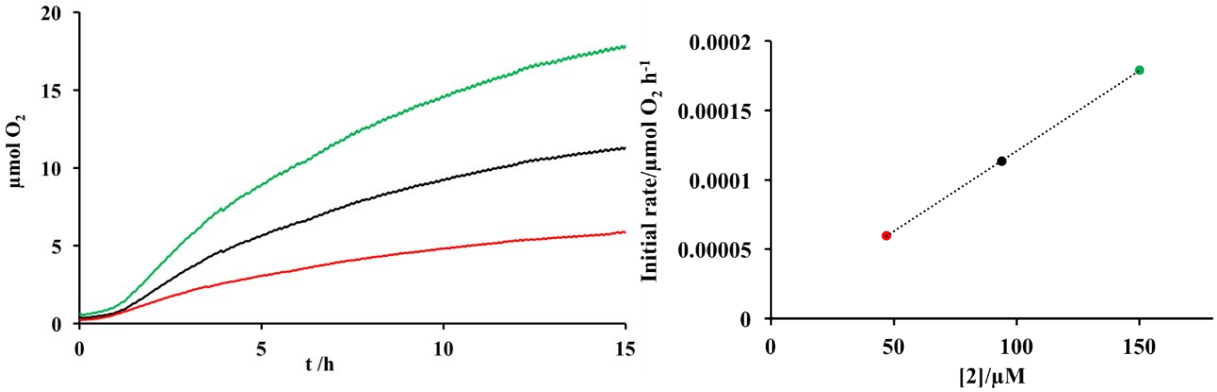

Figure S17. Left side: O_2 evolution *vs* time at different concentration of [**2**]Cl in $HClO_4$ 0.1 M, in presence of CAN (200 mM). Right side: Initial rate of O_2 production as function of catalyst concentration ([**2**]Cl) (47, 94 and 145 μM).

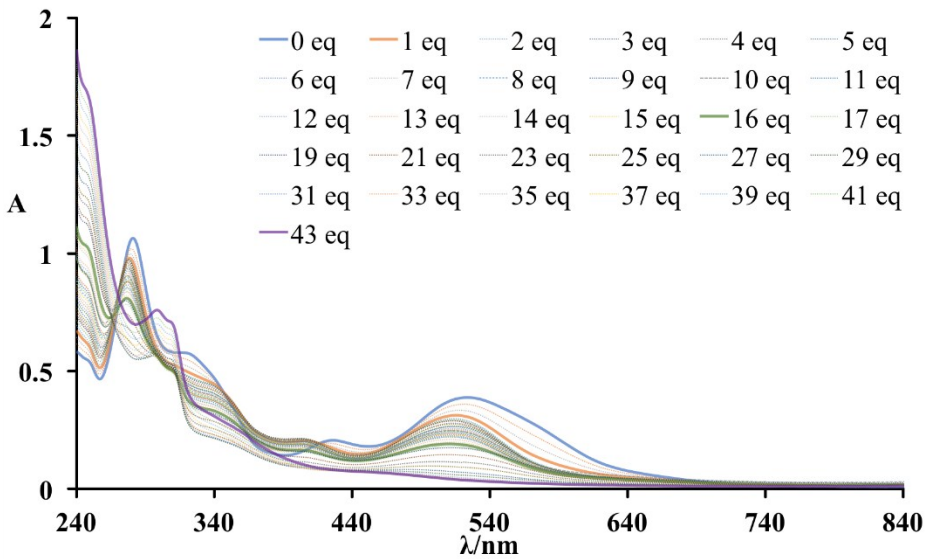

Figure S18. Spectral changes upon addition of CAN (5.2×10^{-3}M) to a solution of [**3**][PF_6]$_3$ (2.5×10^{-5}M) in $HClO_4$ 0.1 M.

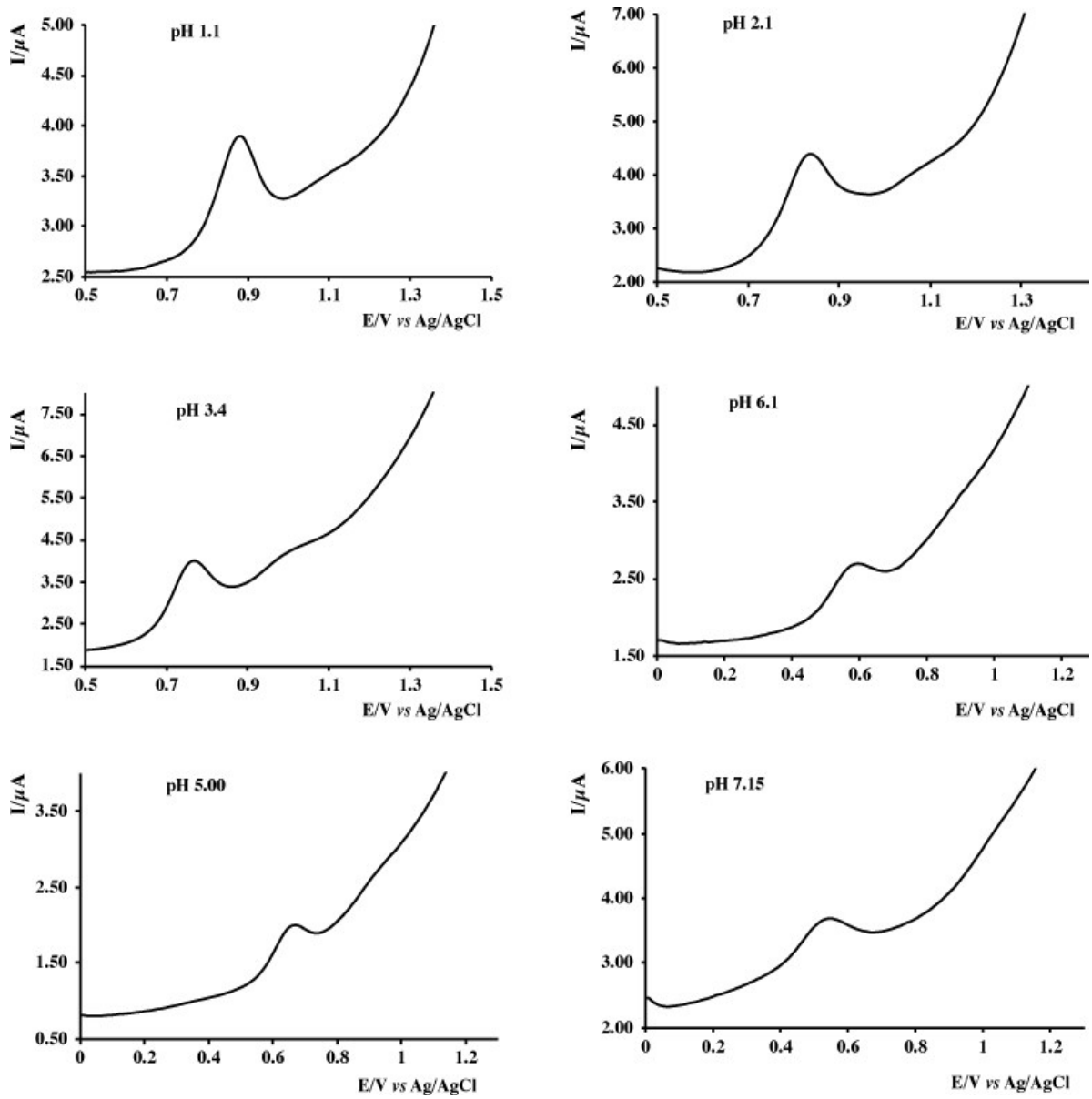

Figure S19. DPV of [**2**]Cl_6 (1.2 x 10^{-4} M) at different pH that were adjusted by adding small amounts of NaOH(s) to a 0.1 M $HClO_4$ solution and determined by a pH-meter. Glassy carbon was used as working electrode, platinum as counter and Ag/AgCl as reference. Scan rate 20 mV/s.

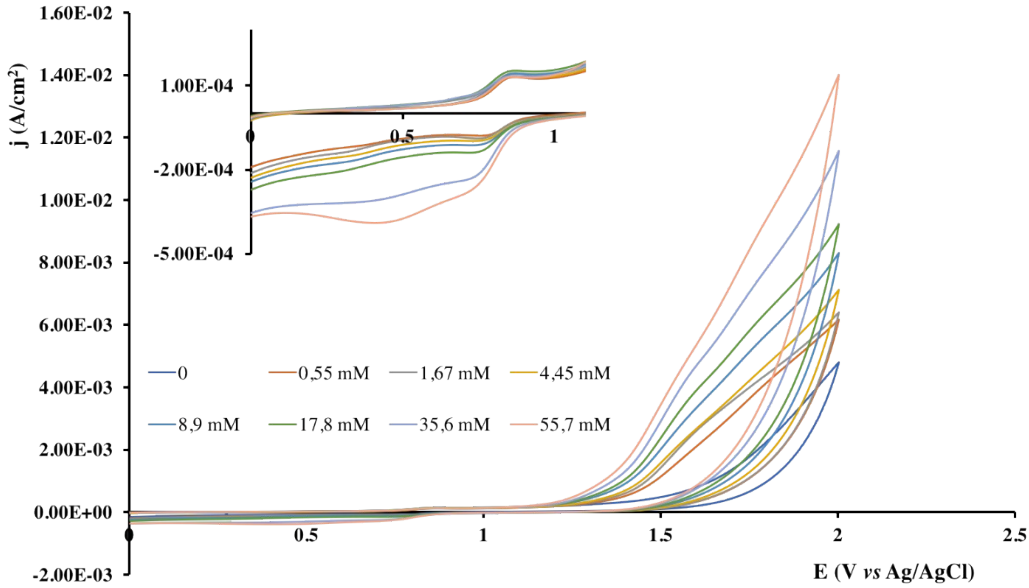

Figure S20. CV of [**2**]Cl (1 mM) in 0.1 M phosphate buffer at pH 7.0 with increasing amounts of NaCl. The inset shows a magnified view in the potential range for the Ru(III/II) and Ru(IV/III) couples. Electrode:glassy carbon; scan rate = 100 mV s^{-1}.

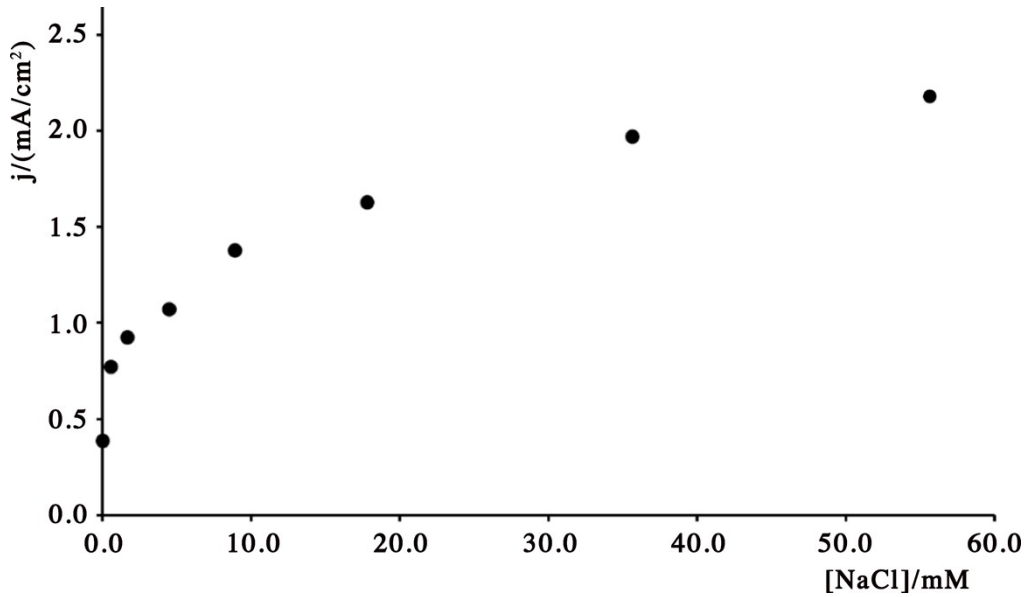

Figure S21. Plot of i_{cat} at 1.65 V vs. [NaCl] for [2]Cl